Pergamon

Polyhedron Vol. 15, No. 24, pp. 4469–4478, 1996
Published by Elsevier Science Ltd
Printed in Great Britain.
0277–5387/96 \$15.00+0.00

S0277–5387(96)00207–0

THE EVALUATION OF SINGLET–TRIPLET SEPARATIONS FOR [$W_2(\mu$-H)(μ-Cl)$Cl_4(\mu$-dppm)$_2$] AND [$W_2(\mu$-H)$_2$ (μ-$O_2CC_6H_5)_2Cl_2(P(C_6H_5)_3)_2$] BASED ON ^{31}P NMR AND CRYSTALLOGRAPHIC DATA

KATHRYN M. CARLSON-DAY, THOMAS E. CONCOLINO and JUDITH L. EGLIN†

Department of Chemistry, Mississippi State University, Mississippi State, MS 39762, U.S.A.

and

CHUN LIN and TONG REN

Department of Chemistry, Florida Institute of Technology, Melbourne, FL 32901, U.S.A.

and

EDWARD J. VALENTE

Department of Chemistry, Mississippi College, Clinton, MS 39058, U.S.A.

and

JEFFREY D. ZUBKOWSKI

Department of Chemistry, Jackson State University, Jackson, MS 39217, U.S.A

(*Received* 9 *February* 1996; *accepted* 23 *April* 1996)

Abstract—The singlet–triplet separations for the edge-sharing bioctahedral (ESBO) complex $W_2(\mu$-H)(μ-Cl)($Cl_4(\mu$-dppm)$_2\cdot$(THF)$_3$ (**II**) has been studied by ^{31}P NMR spectroscopy. The structural characterization of [$W_2(\mu$-H)$_2(\mu$-$O_2CC_6H_5)_2Cl_2(P(C_6H_5)_3)_2$] (**I**) by single-crystal X-ray crystallography has allowed the comparison of the energy of the HOMO–LUMO separation determined using the Fenske–Hall method for a series of ESBO complexes with two hydride bridging atoms, two chloride bridging atoms and the mixed case with a chloride and hydride bridging atom. The complex representing the mixed case, [$W_2(\mu$-H)(μ-Cl)$Cl_4(\mu$-dppm)$_2\cdot$(THF)$_3$] (**II**), has been synthesized and the value of $-2J$ determined from variable-temperature ^{31}P NMR spectroscopy.

Keywords: metal–metal bonds; edge-sharing bioctahedral; single–triplet separation.

The edge-sharing bioctahedral (ESBO) geometry is a familiar one and the study of d^3–d^3 (ESBO) complexes of group VI metals (Cr, Mo and W) has allowed a variety of bonding schemes to be proposed with the resultant bond orders dependent on the nature of the bridging ligands. Based on metal–metal orbital overlap alone, the ordering of

† Author to whom correspondence should be addressed.

the energy levels is $\sigma \ll \pi < \delta < \delta^* < \pi^* < \sigma^*$.[1] However, the bridging ligands influence this ordering to a rather significant degree.[2,3] Many systems with, for example, Cl_2,[4–14] HCl[15–18] or sulfur[1,19] as the bridging ligands have been studied, but no system where two hydride ligands bridge a dinuclear group VI ESBO complex has been previously reported. The first complex of this type, $[W_2(\mu\text{-}H)_2(\mu\text{-}O_2CC_6H_5)_2Cl_2(P(C_6H_5)_3)_2]$ (**I**), has been synthesized. Based on the atomic coordinates of **I** and $[W_2(\mu\text{-}H)(\mu\text{-}Cl)Cl_4(\mu\text{-dppm})_2 \cdot (THF)_3]$ (**II**) determined in crystallographic studies and the coordinates of $[W_2(\mu\text{-}Cl)_2Cl_4(\mu\text{-dppm})_2]$ (**III**) determined in a prior study,[4,15] the electronic structures of **I**, **II** and **III** were evaluated using the Fenske–Hall method for molecular orbital (MO) calculations. Since structural data for a dihydride species are available for the first time, this is the first series where the bridging ligands in ESBO complexes have been varied systematically.[20] Variable-temperature ^{31}P NMR studies were also performed on **II** to obtain the magnitude of the singlet–triplet energy gap $(-2J)$ and the experimental values of $-2J$ for **II** and **III** were compared.[14] Both the experimental studies and the MO calculations confirmed that with small changes in the ligands, changes occur in both the singlet–triplet energy gap and the HOMO–LUMO gap and result in the ability to vary the electronic properties of ditungsten complexes.[2,21]

EXPERIMENTAL

Materials and methods

Standard Schlenk, dry-box and vacuum-line techniques were used employing an argon atmosphere. Commercial-grade THF, toluene and hexanes were dried over potassium/sodium benzophenone ketyl and ethanol was dried over magnesium turnings. All solvents were freshly distilled under a nitrogen atmosphere prior to use. The starting material WCl_4 was synthesized from WCl_6 and $W(CO)_6$ as previously reported.[22] Bis(diphenylphosphino)methane [dppm] was purchased from Strem Chemicals and triphenylphosphine $[PPh_3]$ was purchased from J. T. Baker. Both of these phosphines were kept under dynamic vacuum overnight to remove any residual oxygen or moisture and all subsequent transfers performed under argon. The dinuclear starting materials $W_2(\mu\text{-}O_2CC_6H_5)_4$ and **II** were prepared as previously described.[15,23]

UV–vis absorption spectra were recorded on a Hewlett Packard 8452 model diode array spectrophotometer from 190 to 820 nm. The $^{31}P\ [^1H]$ NMR spectra [162 MHz] were recorded on a General Electric Omega NMR spectrometer with a variable-temperature 10 mm broad band probe and referenced to H_3PO_4. Calibration of the temperature was performed using a methanol sample and the set point did not vary from the actual temperature by more than 1 K over the temperature range 178–295.5 K.[24] When the set point for each temperature was reached during data collection, the sample was allowed to equilibrate for 20 min in the spectrometer. Eleven data points consisting of the temperature and chemical shift were collected over the temperature range 173–238 K for **II**.

$[W_2(\mu\text{-}H)_2(\mu\text{-}O_2CC_6H_5)_2Cl_2(P(C_6H_5)_3)_2]$ (**I**). To unfiltered $W_2(\mu\text{-}O_2CC_6H_5)_4$ (0.200 g, 0.235 mmol) and PPh_3 (0.250 g, 0.953 mmol) in a Schlenk flask was added toluene (14 cm^3). The solution was gently heated for 1 h and a colour change from deep purple to red was observed. A few crystals of the deep red complex were obtained from a toluene solution of the resultant red product layered with ethanol. The chlorine source in the product is derived from the NaCl salt present in the unfiltered $W_2(\mu\text{-}O_2CC_6H_5)_4$ from the reduction of WCl_4 by $NaBEt_3H$.[23] The yield for this reaction was small and incalculable, and we are currently working on a more direct preparative route to complexes of this type.

Computational procedure

Fenske–Hall MO calculations[25] were performed on a VAXstation 4000 VLC. Basis functions used were generated by the numerical Xα atomic orbital program.[26–28]

Model compounds for compounds **I**–**III** were constructed by replacing either PPh_3 or dppm groups with PH_3 where the P—H bond distance is 1.419 Å and the H—P—H bond angle is 93.6° and benzoate with a formate ligand, while the metric parameters about the first coordination sphere of the W_2 core (bond distances and angles) determined by X-ray diffraction study were averaged to an idealized symmetry.[4] Model compounds (effective point symmetry) for **I**, **II** and **III** are, respectively, $W_2(\mu\text{-}H)_2(\mu\text{-}O_2CH)_2(PH_3)_2Cl_2$ (**Im**), (C_{2h}), $W_2(\mu\text{-}H)(\mu\text{-}Cl)(PH_3)_4Cl_4$ (**IIm**), (C_{2v}) and $W_2(\mu\text{-}Cl)_2(PH_3)_4Cl_4$ (**IIIm**), (D_{2h}), which are shown in Fig. 1 along with the master Cartesian coordinates. The master coordinates were chosen so the Z axis is the unique axis of the point symmetry.

Structure determination

X-ray quality crystals of **I** were grown by layering freshly filtered toluene solutions of the compound

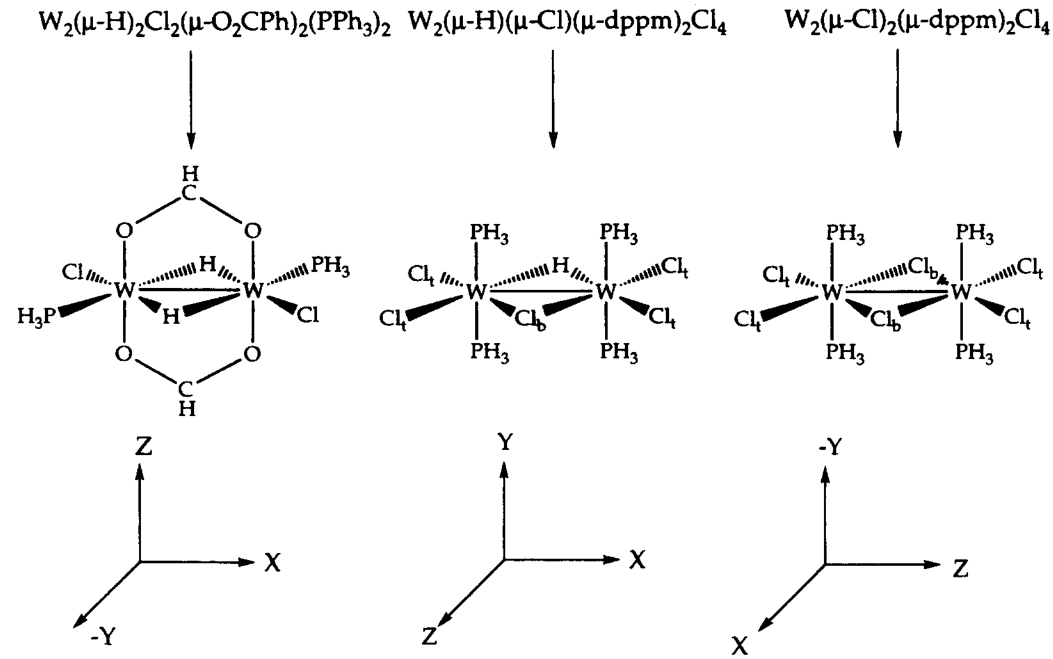

Im **IIm** **IIIm**

Fig. 1. The idealized molecular geometries of C_{2h} symmetry for **Im**, C_{2v} for **IIm** and D_{2h} for **IIIm** generated from X-ray diffraction studies.

with ethanol. A ruby-red cube-like crystal was selected, coated with epoxy cement and mounted on the end of a glass fiber. Data were collected on a Siemens R3m/V automated diffractometer fitted with a molybdenum source and a graphite monochromator. Automatic peak search and indexing procedures yielded a monoclinic reduced primitive cell and inspection of the Niggli values revealed no conventional cell of higher symmetry.

Data were collected using omega scans ($4.04 < 2\theta < 44.94°$). Since a slight decline in the standards of about 4% over the course of the data collection occurred, a correction was applied. Absorption by the small crystal affected reflection intensities by no more than 10% or structure factors by 4% and no correction was applied. The structure was determined by the location of the tungsten atoms in a Patterson function map and the remaining atoms from subsequent difference-Fourier calculation maps.[29–31] The position of H(1) with fixed isotropic vibrational amplitudes was refined. Hydrogen atoms positions on carbon atoms in the ligands were assigned idealized locations. These atoms were included in structure-factor calculations, but not refined.

[$W_2(\mu$-H)(μ-Cl)Cl_4(μ-dppm)$_2\cdot$(THF)$_3$] (**II**) was prepared as previously described and the UV–vis absorption spectrum obtained to confirm the bulk purity of the sample.[15] X-ray quality crystals were grown by layering freshly-filtered THF solutions of the compound with hexanes and the THF solvated structure determined. A blue–green cube–like crystal was selected from a supernatant liquid/mineral oil mixture and mounted in a 0.4 mm capillary. The ends of the capillary were sealed with a small quantity of clay and epoxy cement. Data were collected on a Siemens R3m/V automated diffractometer fitted with a molybdenum source and a graphite monochromator. Automatic peak search and indexing procedures yielded a monoclinic reduced primitive cell and inspection of the Niggli values revealed no conventional cell of higher symmetry.

Data were collected using omega scans ($3.64 < 2\theta < 45°$). No decay was observed on the three standard reflections (0,6,0), (8,0,0) and (0,0,12) over the course of data collection. A slight correction for extinction, 0.00059(4), was applied, but not for absorption since the effect was insignificant in its inclusion. The structure was determined by the location of the tungsten atoms in a Patterson function map and the remaining atoms from subsequent difference-Fourier calculation maps.[29–31]

Other information on the data collection and

Table 1. Crystal data for $[W_2(\mu\text{-}H)_2(\mu\text{-}O_2CC_6H_5)_2Cl_2(P(C_6H_5)_3)_2]$ (**I**) and $[W_2(\mu\text{-}H)(\mu\text{-}Cl)Cl_4(\mu\text{-}dppm)_2\cdot(THF)_3]$ (**II**)

	I	II
Chemical Formula	$C_{50}H_{42}Cl_2O_4P_2W_2$	$C_{50}H_{45}Cl_5P_4W_2\cdot(C_4H_8O)_3$
Formula weight	1207.48	1531.08
Space group	$P2_1/n$ (no. 14)	$P2_1/c$ (no. 14)
a (Å)	10.540(3)	23.630(5)
b (Å)	17.866(7)	12.980(3)
c (Å)	13.284(4)	22.410(4)
β (°)	112.72(3)	114.09(3)
V (Å^3)	2307.4(13)	6275(2)
Z	4	4
ρ_{calc} (g cm^{-3})	1.735	1.557
Crystal size (mm)	0.12 × 0.08 × 0.06	0.4 × 0.4 × 0.3 mm
Wavelength (Å)	0.71073	0.71073
Data collection instrument	R3m/V	R3m/V
Temperature (K)	293(2)	293(2)
Scan method	2 theta	2 theta
Data collection range, 2Θ(°)	4.02–44.94	3.64–45
No. of unique data total:	3006	8183
with $F_o^2 > 2\sigma(F_o^2)$:	1477	5663
Number of parameters refined	275	629
R_1[a]	0.0307	0.0430
wR_2[b]	0.0478	0.1053
Goodness-of-fit indicator	0.462[c]	0.920[c]
Largest shift/e.s.d., final cycle	0.073	0.149
Largest peak (e Å^{-3})	+0.753/−0.835	+2.089/−2.036

[a] $R_1 = \Sigma\|F_o|-|F_c\|/\Sigma|F_o|$.
[b] $wR^2 = \sqrt{(\Sigma[(F_o^2-F_c^2)^2/\Sigma[wF_o^4]})$.
[c] Goodness-of-fit indicator $= [\Sigma(w|F_o|-|F_c|)^2/(n_o-n_v)]^{1/2}$, where n_o = number of observations, n_v = number of parameters and w = weights. $w = 1/[\sigma^2(F_o^2)+(0.0600P)^2+0.15P]$, where $P = (\max(F_o^2,0)+2F_c^2)/3$.

structure solution is provided in Table 1. Selected bond distances and angles for **I** and **II** are provided in Tables 2 and 3, respectively. In addition, a comparison of key bond distances and angles of compounds **I** and **II** to related structures is provided in Table 4.[4,15]

RESULTS AND DISCUSSION

Molecular structures

As shown in Table 4, $[W_2(\mu\text{-}H)_2(\mu\text{-}O_2CC_6H_5)_2Cl_2(P(C_6H_5)_3)_2]$ (**I**) contains the shortest W—W

Table 2. Selected bond distances (Å) and angles(°) for $[W_2(\mu\text{-}H)_2Cl_2(PPh_3)_2(\mu\text{-}O_2CC_6H_5)_2]$ (**I**)

W(1)—W(1a)	2.3500(12)		
W(1)—H(1)	1.67(8)	W(1a)—H(1)	1.90(8)
W(1)—O(1)	2.056(7)	W(1)—O(2)	2.059(6)
W(1)—P(1)	2.576(3)	W(1)—Cl(1)	2.395(3)
O(1)—W(1)—O(2)	177.4(3)	O(1)—W(1)—W(1a)	88.7(2)
H(1)—W(1)—W(1a)	53(2)	H(1)—W(1)—Cl(1)	174(3)
H(1)—W(1)—P(1)	75(2)	O(1)—W(1)—Cl(1)	91.7(2)
O(1)—W(1)—P(1)	84.7(2)	Cl(1)—W(1)—P(1)	101.63(9)
W(1a)—W(1)—Cl(1)	131.26(8)	W(1a)—W(1)—P(1)	126.88(7)
W(1a)—H(1)—W(1)	82(3)		

Table 3. Selected bond distances (Å) and angles (°) for $[W_2(\mu\text{-H})(\mu\text{-Cl})Cl_4(\mu\text{dppm})_2 \cdot (THF)_3]$ (**II**)

W(1)—W(2)	2.4805(7)	W(1)—Cl(1)	2.364(2)
W(1)—Cl(2)	2.443(2)	W(2)—Cl(3)	2.440(2)
W(2)—Cl(4)	2.362(2)	W(1)—Cl(5)	2.477(2)
W(2)—Cl(5)	2.486(2)	W(1)—P(1)	2.550(3)
W(2)—P(2)	2.554(3)	W(1)—P(3)	2.548(3)
W(2)—P(4)	2.558(3)		
Cl(1)—W(1)—W(2)	119.04(7)	Cl(2)—W(1)—W(2)	145.16(7)
Cl(3)—W(2)—W(1)	144.25(7)	Cl(4)—W(2)—W(1)	119.34(7)
W(2)—W(1)—P(1)	95.27(6)	W(1)—W(2)—P(2)	95.63(6)
W(2)—W(1)—P(3)	95.94(6)	W(1)—W(2)—P(4)	94.82(6)
Cl(1)—W(1)—P(3)	81.97(8)	Cl(2)—W(1)—P(3)	87.64(8)
P(3)—W(1)—P(1)	167.01(8)	P(2)—W(2)—P(4)	167.44(8)
Cl(4)—W(2)—Cl(3)	96.39(10)	Cl(1)—W(1)—Cl(2)	95.80(10)
W(1)—Cl(5)—W(2)	59.98(6)		

Table 4. Comparison of selected bond distances and angles for $[W_2(\mu\text{-H})_2Cl_2(PPh_3)_2(\mu\text{-}O_2CC_6H_5)_2]$, $[W_2(\mu\text{-Cl})(\mu\text{-H})Cl_4(\mu\text{-dppm})_2 \cdot (THF)_3]$, $W_2(\mu\text{-Cl})(\mu\text{-H})Cl_4(\mu\text{-dppm})_2$ and $W_2(\mu\text{-Cl})_2Cl_4(\mu\text{-dppm})_2$

Compound	W—W bond distance (Å)	W—bridge bond distance (Å)	W—bridge—W bond angle (°)	W—W—Cl bond angles (°)
$[W_2(\mu\text{-H})_2Cl_2(PPh_3)_2(O_2CC_6H_5)_2]$	2.3500(12)	1.67(8) 1.90(8)	82(3)	131.26(8)
$[W_2(\mu\text{-Cl})(\mu\text{-H})Cl_4(dppm)_2 \cdot (THF)_3]$	2.4805(7)	2.477(2) 2.486(2)	59.98(6)[a]	144.25(7)[a] 145.16(7)[a] 119.04(7) 119.34(7)
$W_2(\mu\text{-Cl})(\mu\text{-H})Cl_4(dppm)_2$[15]	2.4830(9)	2.470(4) 2.486(5)	60.1(1)	144.9(1)[a] 145.9(1)[a] 119.7(1) 119.8(1)
$W_2(\mu\text{-Cl})_4(dppm)_2$[4]	2.691(1)	2.405(3) 2.393(3)	68.23(9)	137.65[b]

[a] Side of molecule with bridging chloride.
[b] Calculated value.

bond distance, 2.3500 (12) Å, in the series $W_2(\mu\text{-}X)_2Cl_4(\mu\text{-dppm})_2$. This bond distance is 0.13 Å shorter than the W—W bond distance in $[W_2(\mu\text{-H})(\mu\text{-Cl})Cl_4(\mu\text{-dppm})_2 \cdot (THF)_3]$ (**II**). Only minor changes in the structure of **II** occur due to the presence of the THF solvent in the crystal lattice.[15] An ORTEP drawing of **I** is shown in Fig. 2 and the structure of **II** including the THF molecules in the crystal lattice is shown in Fig. 3. The bond distances in **I**, a triply bonded ESBO compound, is only 0.08 Å longer than the W—W bond distance in the quadruply bonded compound $W_2Cl_4(\mu\text{-dppm})_2$ and 0.036 Å longer than the W—W bond distance observed in $\beta\text{-}W_2Cl_4(\mu\text{-dppe})_2$.[32,33] However, **I** does contain a W—W bond distance that is slightly longer than the W—W bond distances observed in the Chisholm type triply bonded compounds.[34,35] The W—Cl, W—O and W—P bond distances fall within the expected ranges based on other ditungsten compounds and the bulky PPh_3 ligands are *trans* to one another, as one would predict for steric reasons.[23]

Also of note in the structure of this dihydride compound are the W—W—Cl_t and W—W—P_t bond angles of 131.26 and 126.88°, respectively. (The subscripts t and b as labels refer to terminal and bridging atoms, respectively, in ESBO complexes.) The angles are 7–11° more acute than the angle in $[W_2(\mu\text{-Cl})_2Cl_4(\mu\text{-dppm})_2]$, but extremely close to the angle predicted by the

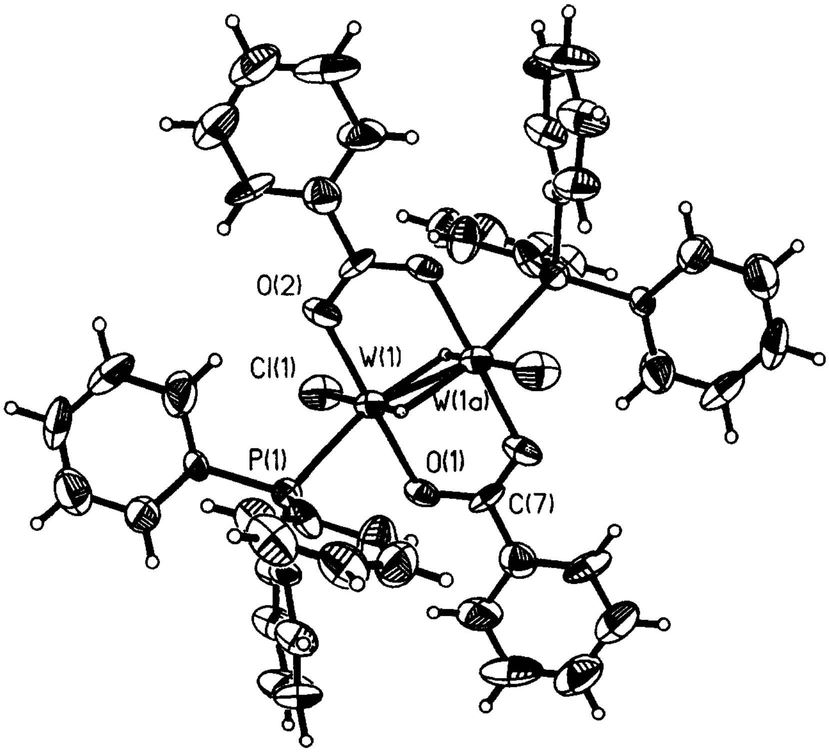

Fig. 2. A thermal ellipsoid plot of $[W_2(\mu\text{-}H)_2Cl_2(PPh_3)_2(O_2CC_6H_5)_2]$ (**I**). Thermal ellipsoids for W, Cl, P, O and C are shown at 50% probability. The hydrogen atoms are as arbitrarily sized uniform circles.

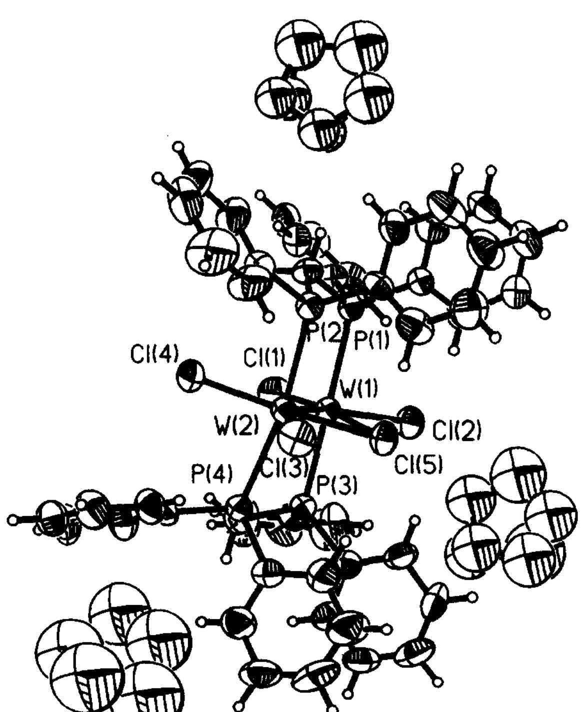

Fig. 3. A thermal ellipsoid plot of $[W_2(\mu\text{-}Cl)(\mu\text{-}H)Cl_4(dppm)_2 \cdot (THF)_3]$ (**II**). Thermal ellipsoids for W, Cl, P, O and C are shown at 50% probability. The hydrogen atoms are shown as arbitrarily sized uniform circles.

orbitals alone. Optimally the two terminal ligands would form a 90° angle with each bonding to the metal centre through a lobe of the d_{xy} orbital (as defined for **Im**). By simply dividing the remaining 270° by two based on the symmetry of the molecule, one would predict a 135° angle for W—W—Cl_t with *trans* Cl_b—W—Cl_t or H_b—W—Cl_t angles of 180° for $[W_2(\mu\text{-}Cl)_2Cl_4(\mu\text{-}dppm)_2]$ or $[W_2(\mu\text{-}H)_2Cl_4(\mu\text{-}dppm)_2]$. While the W—W—$Cl_t$ angle in **I** is slightly smaller than 135°, the presence of bulky PPh_3 ligands results in a large Cl_t—W—P_t bond angle for the terminal ligands, 101.63° and a slight asymmetry of the W—H bond distances is observed.

Based on this simple bonding picture, one would predict that ESBO molecules with equivalent bridging groups would have M—M—Cl_t angles extremely close to 135° when the terminal chlorides or other halides are in the same plane as the bridging groups. As shown in Table 4, the angle observed in **III** is 138°, quite similar to the predicted value. In fact, for the series $[M_2(\mu\text{-}Cl)_2Cl_4(\mu\text{-}dppm)_2]$, where M is Nb, Ta, Mo, Re and Ru, deviations of no more than 4.12° (Re) from the optimal value of 135° are observed in the M—M—Cl_t angles.[8] Even for the mixed-metal compound, $MoW(\mu\text{-}Cl)_2Cl_4(\mu\text{-}dmpm)_2$, M—M—$Cl_t$ angles of 138.8(1) and 136.8(1)° are observed.[14]

Replacement of dppm with monodentate ligands in $[Mo_2(\mu\text{-}Cl)_2Cl_4(PMe_2Ph)_4]$ does not change this angle sufficiently. For terminal halides in the same plane as the bridging halides, Mo—Mo—Cl_t angles of 136.93(4) and 136.65(4)° are observed.[9] In the acetonitrile complex $[W_2Cl_4(\mu\text{-dppm})_2(\eta^2\text{-}\mu\text{-}CH_3CN)]$ one would also expect a W—W—Cl_t angle of 135° with no asymmetry of the metal to bridging bond distances to cause a distortion. Indeed the W—W—Cl_t angles are 136.82(6), 134.70(6), 135.15(5) and 136.62(6)° for $W_2Cl_4(\mu\text{-dppm})_2(\eta^2\text{-}\mu\text{-}CH_3CN)$.[36]

This implies that the asymmetry of the W—H_b and W—Cl_b bond distances in $[W_2(\mu\text{-H})(\mu\text{-Cl})Cl_4(\mu\text{-dppm})_2]$ causes a significant distortion of the W—W—Cl_t angles instead of steric interactions. In Fig. 4 the bond distances shown have been obtained from the structure of **III** with equivalent bridging atoms and $[W_2(\mu\text{-H})(\mu\text{-Cl})Cl_2[P(n\text{-}Bu)_3]_2[C_6H_5CO_2]_2]$ to reflect the mixed case with a chloride and hydride bridging atom.[4,18] One could imagine the asymmetry observed in **II** and related $(\mu\text{-H})(\mu\text{-Cl})$ compounds resulting from one of the M—X_b distances being significantly shorter than the other, distorting the molecule while retaining *trans*-X_b—M—X_t angles close to 180°.[16,18,37] While the W—H_b bond distance for **II** has not been determined from crystallographic data, the W—H_b [1.534(1) Å] and W—Cl_b [2.454(6) Å] bond distances shown in Fig. 4 were obtained for the compound $[W_2(\mu\text{-H})(\mu\text{-Cl})Cl_2[P(n\text{-}Bu)_3]_2[C_6H_5CO_2]_2]$.[18] The W—$Cl_b$—W angle in $[W_2(\mu\text{-H})(\mu\text{-Cl})Cl_2[P(n\text{-}Bu)_3]_2[C_6H_5CO_2]_2]$ is more acute, 58.9(2)°, than either **I** or **III** with W—H_b—W and W—Cl_b—W angles of 82(3) and 68.23(9)°, respectively.[4] While the W—Cl_b—W angle in $[W_2(\mu\text{-H})(\mu\text{-Cl})Cl_2[P(n\text{-}Bu)_3]_2[C_6H_5CO_2]_2]$ is more acute, the W—H_b—W angle is more obtuse, 108.69(6)°, due to the asymmetry in the bridging atoms.[18] This distortion results M—M—Cl_t angles of approximately 119° for Cl_t *trans* to the Cl_b and 145° for Cl_t *trans* to the H_b in the case of $(\mu\text{-H})(\mu\text{-Cl})$ complexes.[16,18,37]

Electronic structures

In model compounds **Im**–**IIIm**, there are 39, 41 and 43 occupied valence molecular orbitals, respectively. Most of the low-energy valence orbitals are either intraligand bonding orbitals or W—L σ-bonding orbitals, and they are omitted from the discussion. High-energy valence orbitals of dominant tungsten character are summarized in Table 5.

In the model compound **Im**, $[W_2(\mu\text{-H})_2(\mu\text{-O}_2CH)_2$

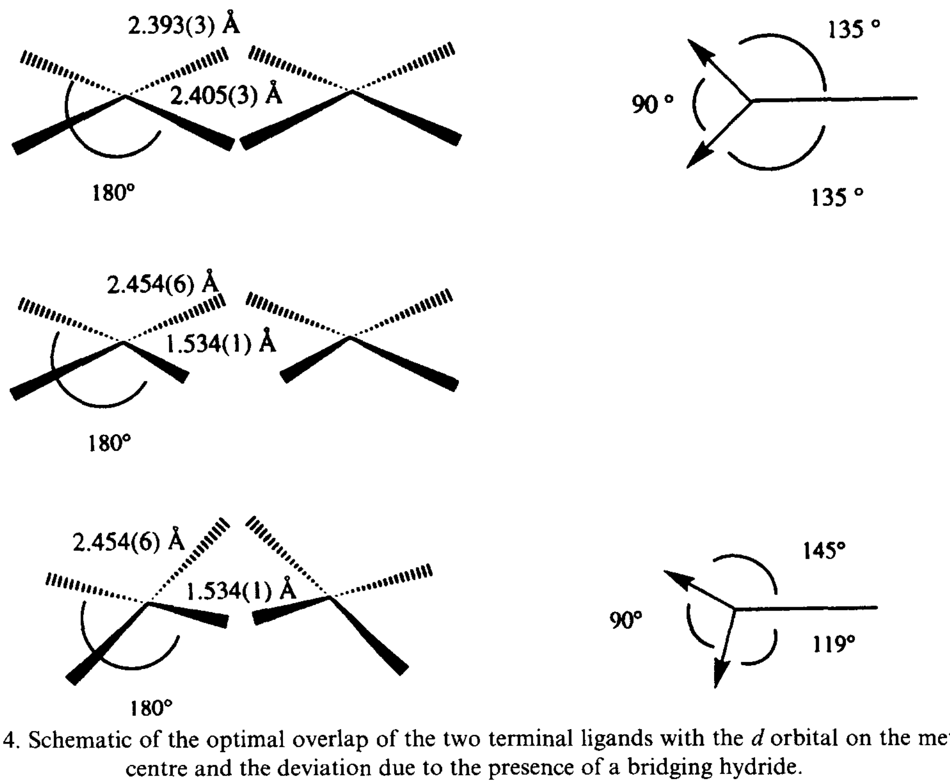

Fig. 4. Schematic of the optimal overlap of the two terminal ligands with the *d* orbital on the metal centre and the deviation due to the presence of a bridging hydride.

$(PH_3)_2Cl_2]$, the W—W bonding and antibonding molecular orbitals in order of the ascending energy are $13a_g(\sigma)$, $8a_u(\pi_{xz})$, $7b_g(\delta$, HOMO), $12b_u(\sigma^*$, LUMO), $9a_u(\delta^*)$ and $8b_g(\pi_{xz}{}^*)$. On the basis of the orbital occupancy and the large HOMO–LUMO gap (2.7 eV), a W—W triple bond exists $(\sigma^2\pi^2\delta^2)$, which is consistent with the short W—W bond length found in the X-ray structural determination, 2.3500(12)Å. The d_{xy} orbitals, on which an additional W—W π-bond would be based in the absence of bridging hydrides, are extensively involved in the W—H σ-bonding. However, the lack of π-donor orbitals on the bridging hydrides led to the full retention of the W—W δ-bonding orbital. Compound **I** is expected to be diamagnetic based on the significant HOMO–LUMO gap derived from the model calculation.

In model compounds **IIm**, $[(W_2(\mu\text{-H})(\mu\text{-Cl})(PH_3)_4Cl_4)]$, the high-energy orbitals of dominant W contributions are $8b_2$ (π_{xy}), $14a_1$, $9b_2$ (δ, HOMO), $7a_2$ (δ^*, LUMO) and $12b_1$, $8a_2$ (π^*_{xy}). The δ and δ^* orbitals are separated by only 0.41 eV, which, upon inspecting the orbital populations, results from the destabilization of the δ-orbital by the lone-pair electrons of both the bridging and the terminal Cl ligands. Nevertheless, the normal $E(\delta) < E(\delta^*)$ order is retained since such destabilization is (i) less dramatic than that in the dichloro-bridged compound (see below) and (ii) countered by a strong δ-bonding overlap due to the relatively short W—W distance. In addition to the δ-orbital, π_{xy} is the other unambiguous W—W bonding orbital. A W—W σ-bond is also possible, since there are many low-energy bonding orbitals (all of a_1 symmetry) containing significant ($\geqslant 10\%$) $d_{x^2-y^2}$ contribution. Therefore, a formal triple-bond configuration $(\sigma^2\pi^2\delta^2)$† is tentatively assigned. However, as noted earlier, the W—W bond length in **II** is significantly

Table 5. Upper valence moelcular orbitals for the model compounds **Im**–**IIIm**

Symbol	E(eV)	Assignment	Characters (%)
$W_2(\mu\text{-H})_2(\mu\text{-formate})_2(PH_3)_2Cl_2$ (**Im**)			
$14a_g$	5.36	W—μ—H $s(nb)$	W d_{xy} (65), p (20)
$13b_u$, $9b_g$	1.83, 0.96	C—O σ^*	C (62); O (37)
$8b_g$	0.56	W—W $\pi^*(xz)$	W d_{xz} (87)
$9a_u$	−2.92	W—W δ^*	W d_{yz} (84), O p_π (10)
$12b_u$	−3.54	W—W σ^*, LUMO	W $d_{x^2-y^2}$ (68), p_x (11); Cl (10)
$7b_g$	−6.21	W—W δ, HOMO	W d_{yz} (81); C (10)
$8a_u$	−7.43	W—W $\pi(xz)$	W d_{xz} (79); Cl p (11)
$13a_g$	−7.88	W—W σ; W—L σ	W $d_{x^2-y^2}$ (55); Cl p (33); H_b (5)
$W_2(\mu\text{-H})(\mu\text{-Cl})(PH_3)_4Cl_4$ (**IIm**)			
$14b_1$	8.88	W—W σ^*; W—L σ^*	W, $d_{x^2-y^2}$ (44), d_{z^2} (11); Cl p (16); P (20)
$15a_1$	8.47	W—L σ^*	W, d_{z^2} (30), $d_{x^2-y^2}$ (16), d_{xz} (13); Cl_b (13); P (16)
$13b_1$	5.05	W—W $\pi^*(xz)$	W d_{xz} (52), p_z (17), d_{z^2} (11); Cl (15)
$8a_2$	−2.11	W—W $\pi^*(xy)$	W d_{xy} (91)
$12b_1$	−2.75	W—W σ^*, W—L σ^*	W d_{z^2} (45), d_{xz} (21), $d_{x^2-y^2}$ (10); Cl_b, (6); Cl_t (10)
$7a_2$	−5.76	W—W δ^*, LUMO	W d_{yz} (83); Cl_t, p (15)
$9b_2$	−6.17	W—W δ, HOMO	W d_{yz} (72); Cl_b, p (9); Cl_t, p (14)
$14a_1$	−8.54	W—W σ; W—Cl σ	W d_{z^2} (29), $d_{x^2-y^2}$ (18), d_{xz} (6); Cl p (44)
$8b_2$	−8.90	W—W $\pi(xy)$	W d_{xy} (53); Cl_{trans} p (38)
$W_2(\mu\text{-Cl})_2(PH_3)_4Cl_4$ (**IIIm**)			
$6b_{2g}$	5.59	W—Cl_b—W, σ^*	W d_{xz} (68); Cl p (28)
$8b_{1u}$	0.37	W—W σ^*	W d_{z^2} (53), $d_{x^2-y^2}$ (22); Cl_b (18)
$5b_{3g}$	−3.83	W—W $\pi^*(yz)$	W d_{yz} (89); Cl_t (8)
$3b_{1g}$	−5.21	W—W δ, LUMO	W d_{xy} (77); Cl_b, p (12); Cl_t, p (10)
$3a_u$	−6.38	W—W δ^*, HOMO	W d_{xy} (81); Cl_t, p_x (16)
$6b_{2u}$	−7.50	W—W $\pi(yz)$,	W d_{yz} (67); Cl lone pairs (31)
$9a_g$	−8.42	W—W σ	W d_{z^2} (52), $d_{x^2-y^2}$ (10), p_z (4)

longer than that in **I**, an authentic triply-bonded compound. The elongation of W—W bond originates, in part, from the small $\delta-\delta^*$ gap, which enables a low-energy triplet excited state ($\delta\delta^*$) that is significantly populated at ambient temperature and leads to partial cancellation of δ-bonding.

In model compound **IIIm**, $[W_2(\mu\text{-Cl})_2(PH_3)_4Cl_4]$, the molecular orbital with significant tungsten contributions in order of the ascending energy are $9a_g(\sigma)$,$6b_{2u}(\pi_{yz})$, $3a_u(\delta^*,\text{HOMO})$, $3b_{1g}(\delta,\text{LUMO})$, $5b_{3g}(\pi^*_{yz})$, $8b_{1u}(\sigma^*)$ and $6b_{2g}$(W—Cl_b—W σ^*). Hence, the model calculation indicates a W—W bonding configuration $\sigma^2\pi^2\delta^{*2}$, which is interpreted as a strong single W—W bond. Comparing the characters of δ-orbital in **IIm** and **IIIm**, the only substantial difference is the contribution from the lone-pair donor orbital of bridging chloride(s), which increases from 8% in **IIm** to 12% in **IIIm**. This increased antibonding interaction and the reduced direct overlap between d_{xy} orbitals due to the elongation of W—W bond result in $E(\delta^*) < E(\delta)$, in contrast to the order observed for **IIm**, $E(\delta) < E(\delta^*)$. Although the SCF iteration converged with a closed-shell configuration and a sizable δ^*-δ gap (1.17 eV), the actual gap may be much smaller due to both the nature of SCF method and some crude approximations in the Fenske–Hall procedure. When this factor is taken into consideration, the MO calculation does not necessarily conflict with the observed paramagnetism of **III**. In order to account for the paramagnetism of **III**, the δ-orbital must be thermally populated and the resulting bond order is two ($\sigma^2\pi^2\delta^{*1}\delta^1$). However, the Fenske–Hall calculations do predict a smaller HOMO–LUMO gap for compound **II** relative to compound **III**.

^{31}P NMR spectroscopy and further discussion of bonding

Although the ordering of the energy levels in d^3–d^3 systems with ESBO geometries is $\sigma \ll \pi < \delta < \delta^* < \pi^* < \sigma^*$ based on W—W overlap alone,[1] the bridging ligands influence this ordering to a rather significant degree as confirmed by our Fenske–Hall calculations for the model systems **Im**, **IIm** and **IIIm** and other bonding studies. As a result, the system described by **III** with two bridging halide ligands has the following orbital ordering $\sigma \ll \pi < \delta^* < \delta < \pi^* < \sigma^*$.[2,3]

The small energy separation between the δ and δ^* orbital in ESBO molecules usually leads to a thermally accessible singlet [$^1(\delta^2)$ or $^1(\delta^{*2})$] -triplet [$^3(\delta\delta^*)$] gap, $-2J$, which is reflected in the temperature-dependent paramagnetism of these molecules. This magnetic behaviour is observed in the NMR spectra and the magnetic susceptibility data of these compounds as an extremely temperature-dependent chemical shift or an increase in the paramagnetism of the complexes as higher temperatures are approached.[5–7,9,10,12–14,38] Variable-temperature ^{31}P NMR spectroscopy has been used successfully to determine the $-2J$ value in both edge-sharing bioctahedral complexes and quadruply-bonded complexes of dimolybdenum and tungsten.[13,14,39] A HUMO–LUMO gap of 0.595 eV has been determined for $[Mo_2(\mu\text{-Cl})_2Cl_4(\mu\text{-dppm})_2]$, based on extended Huckel MO calculations[2] and variable-temperature ^{31}P NMR data has been used to obtain the value of the singlet–triplet gap in the molecule, 1460 cm^{-1}.[8,14]

Using eq. (1):

$$H_{\text{obs}} = H_{\text{dia}} + \frac{2g\beta H_{0(N)}A}{(\gamma_{(N)}/2\pi)kT}(3+e^{2J/kT})^{-1}$$

where $\gamma_{(N)}$ is the gyromagnetic ratio of the nucleus (N), $H_{0(N)}$ is the resonance frequency, g is the Lande' splitting factor and β the Bohr magneton for the electron, the equation was fit to the temperature-dependent ^{31}P NMR data (H_{obs} versus T) to determine H_{dia}, the diamagnetic resonance frequency of the nucleus, the singlet–triplet gap, and A, the hyperfine coupling constant.[13,14,39,40–44] However, it is worthwhile to point out that the magnitude of $-2J$ is merely the energy separation between the singlet and the triplet configuration and does not reveal the nature of the ground state singlet configuration, $^1(\delta^2)$ or $^1(\delta^{*2})$.

A significant decrease of the singlet–triplet gap is observed upon replacement of a bridging chloride with a bridging hydride. For **II**, the singlet–triplet gap determined by a exponential curve fit to the data over the temperature range 173 to 238 K is 864 ± 12 cm^{-1} with a H_{dia} of -15 ± 1 ppm. In contrast, the dichloro-bridged complex **III** has a larger singlet–triplet separation of 1230 cm^{-1}.[14]

Stepwise substitution of Cl with H at the bridging positions gradually reduces the destabilization of the W—W δ-bonding orbital as reflected in both the results of the Fenske–Hall calculations and the singlet–triplet gap determined by variable-temperature ^{31}P NMR studies. The maximum stability

† SCF iteration also converged with both δ and δ^* half-filled by allowing pseudo-degeneracy ($\Delta E \leqslant 0.5$ eV). The resulting $\delta-\delta^*$ gap was 0.43 eV and there is no significant change in both energies and populations for all of the upper valence MOs. See *Fenske–Hall Input Instructions*, Version 5.1 (Professor Michael B. Hall, Texas A&M University, 1989) for details.

of the δ bond is reached with dihydrido species **I**, where the model calculation confirmed the formation of a W—W triple bond and predicted a diamagnetic molecule based on the large HUMO–LUMO gap (2.67 eV). When bulk quantities of **I** or a analogous ESBO compound are made, the ^{31}P NMR spectra should have no temperature dependence. A more direct, bulk synthetic method for compounds of this type is currently being pursued.

Supplementary material. Listing of observed and calculated structure factors (26 pages) and complete tables of crystal data, positional and isotropic equivalent thermal parameters, anisotropic thermal parameters, bond distances, and bond angles for molecules **I** and **II** (19 pages) are available from author J.L.E. upon request.

Acknowledgements—Authors J. Elgin, K. Carlson-Day and T. Concolino would like to acknowledge the support of the National Science Foundation EPSCoR program (Grant No. EHR 9108767 and OSR 9452857), the ARI Program (Grant No. CHE-92-14521), the donors of The Petroleum Research Fund, administered by the ACS, for partial support of this research and Dr Thomas Cundari and the reviewers for helpful suggestions. Authors E. Valente and J. Zubkowski acknowledge the support of the Office of Naval Research.

REFERENCES

1. F. A. Cotton, *Polyhedron* 1987, **6**, 667.
2. R. Poli and R. C. Torralba, *Inorg. Chim. Acta* 1993, **212**, 123.
3. C. R. Fisel, R. Hoffman, S. Shaik and R. Summerville, *J. Am. Chem. Soc.* 1980, **102**, 4555.
4. J. M. Canich, F. A. Cotton, L. M. Daniels and D. B. Lewis, *Inorg. Chem.* 1987, **26**, 4046.
5. F. A. Cotton, J. L. Eglin, R. L. Luck and K. Son, *Inorg. Chem.* 1990, **29**, 1802.
6. H. D. Mui and R. Poli, *Inorg. Chem.* 1989, **28**, 3609.
7. P. A. Agaskar, F. A. Cotton, K. R. Dunbar, L. R. Falvello and C. J. O'Conner, *Inorg. Chem.* 1987, **26**, 4051.
8. A. R. Chakravarty, F. A. Cotton, M. P. Diebold, D. B. Lewis and W. J. Roth, *J. Am. Chem. Soc.* 1986, **108**, 971.
9. R. Poli and H. D. Mui, *Inorg. Chem.* 1991, **30**, 65.
10. H. Rothfuss, J. T. Barry, J. C. Huffman, K. G. Caulton and M. H. Chisholm, *Inorg. Chem.* 1993, **32**, 4573.
11. R. B. Jackson and W. E. Streib, *Inorg. Chem.* 1971, **10**, 1760.
12. F. A. Cotton, J. Su, Z. S. Sun and H. Chen, *Inorg. Chem.* 1993, **32**, 4871.
13. F. A. Cotton, J. L. Eglin, B. Hong and C. A. James, *J. Am. Chem. Soc.* 1992, **114**, 4915.
14. F. A. Cotton, J. L. Eglin, C. A. James and R. L. Luck, *Inorg. Chem.* 1992, **31**, 5308.
15. P. Fanwick, W. S. Harwood and R. A. Walton, *Inorg. Chem.* 1987, **26**, 242.
16. F. A. Cotton, C. A. James and R. L. Luck, *Inorg. Chem.* 1991, **30**, 4370.
17. R. T. Carlin and R. E. McCarley, *Inorg. Chem.* 1989, **28**, 2604.
18. F. A. Cotton and G. N. Mott, *J. Am. Chem. Soc.* 1982, **104**, 5978.
19. K. A. Hall and J. M. Mayer, *Inorg. Chem.* 1995, **34**, 1145.
20. R. Summerville and R. Hoffmann, *J. Am. Chem. Soc.* 1979, **101**, 3821.
21. M. D. Fryzuk, D. B. Leznoff, S. J. Rettig and R. C. Thompson, *Inorg. Chem.* 1994, **33**, 5528.
22. M. A. S. King and R. E. McCarley, *Inorg. Chem.* 1973, **12**, 1972.
23. K. M. Carlson-Day, J. L. Eglin, E. J. Valente and J. D. Zubkowski, *Inorg. Chim. Acta* 1996, **224**, 151.
24. A. L. VanGeet, *Anal. Chem.* 1970, **42**, 679.
25. M. B. Hall and R. F. Fenske, *Inorg. Chem.* 1972, **11**, 768.
26. F. Herman and S. Skillman, *Atomic Structure Calculations*. Prentice-Hall, Englewood Cliffs, New Jersey (1963).
27. B. E. Bursten, J. R. Jensen and R. F. Fenske, *J. Chem. Phys.* 1978, **68**, 3320.
28. B. E. Bursten and R. F. Fenske, *J. Chem. Phys.* 1977, **67**, 3138.
29. *International Tables for X-ray Crystallography*. D. Reidel Publishing, Dordrecht, Netherlands (1985).
30. G. M. Sheldrick, *Acta Cryst.* 1990, **A46**, 467.
31. G. M. Sheldrick, *Crystallographic Computing*. Oxford University Press, Oxford. U.K. (1992).
32. J. M. Canich and F. A. Cotton, *Inorg. Chim. Acta* 1988, **142**, 69.
33. F. A. Cotton and T. Felthouse, *Inorg. Chem.* 1981, **20**, 3880.
34. K. J. Ahmed, M. H. Chisholm, K. Folting and J. C. Huffman, *Inorg. Chem.* 1985, **24**, 4039.
35. A. Akiyama, M. H. Chisholm, F. A. Cotton, M. W. Extine, D. A. Haitko, D. Little and P. E. Fanwick, *Inorg. Chem.* 1979, **18**, 2266.
36. J. L. Eglin, E. M. Hines, E. J. Valente and J. D. Zubkowski, *Inorg. Chim. Acta* 1995, **229**, 113.
37. P. E. Fanwick, W. S. Harwood and R. A. Walton, *Inorg. Chem.* 1987, **26**, 242.
38. F. A. Cotton, M. P. Diebold, C. J. O'Connor and G. L. Powell, *J. Am. Chem. Soc.* 1985, **107**, 7438.
39. F. A. Cotton, J. L. Eglin, B. Hong and C. A. James, *Inorg. Chem.* 1993, **32**, 2104.
40. M. D. Hopkins, H. B. Gray and V. M. Miskowski, *Polyhedron* 1987, **6**, 705.
41. A. D. Boersma, M. A. Phillipi and H. M. Goff, *J. Magn. Res.* 1984, **57**, 197.
42. R. H. Holm and C. J. Hawkins, *NMR of Paramagnetic Molecules*. Academic Press, New York (1973).
43. G. C. Campbell and J. F. Haw, *Inorg. Chem.* 1988, **27**, 3706.
44. G. C. Campbell, J. H. Reibenspies and J. F. Haw, *Inorg. Chem.* 1991, **30**, 171.